III-V-on-Si DFB Laser With Co-Integrated Power Amplifier Realized Using Micro-Transfer Printing

Jing Zhang, Laurens Bogaert, Bahawal Haq, Ruohui Wang, Bozena Matuskova, Johanna Rimböck, Stefan Ertl, Agnieszka Gocalinska, Emanuele Pelucchi, Brian Corbett, Joris Van Campenhout, *Member, IEEE*, Guy Lepage, Peter Verheyen, Geert Morthier, *Senior Member, IEEE*, and Gunther Roelkens, *Senior Member, IEEE*

***Abstract*— A C-band III-V-on-Si distributed feedback (DFB) laser with co-integrated power amplifier was realized using micro-transfer printing. The DFB laser exhibits single mode operation around 1540 nm at 20 °C. By driving the DFB laser and co-integrated power amplifier simultaneously, up to 14 dBm waveguide-coupled output power with over 28 dB side mode suppression ratio was achieved at an overall bias current of 270 mA.**

***Index Terms*— III-V-on-Si integration, DFB laser, integrated power amplifier, micro-transfer printing.**

I. Introduction

Silicon photonics (SiPh) has experienced a rapid development in the past decades. Photonic integrated circuits (PICs) realised on different SiPh platforms have found their use in a wide range of applications. By leveraging the well-established CMOS fabrication infrastructure and mature semiconductor processes, today these PICs can be manufactured on 200 mm and 300 mm silicon-on-insulator (SOI) wafers in high-volume and with a high yield. With a variety of high-performance readily available building blocks, one can design and realize complex SiPh circuits with compact footprints thanks to the high index contrast of Si to SiO_2 [1]. However, several essential functionalities, such as optical gain, optical source, integrated isolators and circulators, are still missing on these SiPh platforms. Different approaches have been developed to address this issue by combining the SiPh circuit with other materials that can realize those desired functionalities. Amongst these approaches, multi-die-to-wafer bonding allows for wafer-scale integration of III-V-on-Si devices and has been successfully developed for the manufacturing of optical transceiver modules with heterogeneously integrated III-V-on-Si lasers [2]. This comes however at the cost of substantial modifications to the established SiPh back-end process flow and therefore requires vast capital investment. Meanwhile, hetero-epitaxial growth is acknowledged as the ultimate solution, but it is still in an early stage and many fundamental issues need to be addressed first [3]. Micro-transfer printing (μTP) is another III-V-on-Si integration approach that holds great potential and has attracted major interest from both academia and industry [4]. It not only allows for wafer-scale integration of microscale-sized opto-electronic device coupons and material films, but also requires minimal disruption to the SiPh process flow. Dedicated processes have been developed to enable the release and printing of a variety of opto-electronic components in different material systems. These include, but are not limited to, III-V amplifiers [5], lasers [6], [7], micro-LEDs [8], III-V photodiodes [9], [10], [11], [12], Ge PDs [13], crystalline Si coupons [14], $LiNbO_3$ film coupons [15], [16] and even (high-speed) electronics circuits [17].

The first micro-transfer-printed electrically pumped III-V-on-Si DFB laser is based on the transfer printing of III-V material film coupons [18]. Single mode operation was demonstrated in this work, but this approach requires complicated process steps on the target substrate. Recently, B.Haq et al. demonstrated single mode DFB lasers by transfer printing pre-fabricated III-V taper structures on Si PICs defined in a 400 nm thick device layer with a 50 nm thick PECVD SiN overlay layer where a first-order quarter wave shifted Bragg grating was patterned using e-beam lithography [19]. In this paper, we demonstrate a C-band

Manuscript received 30 January 2023; accepted 21 March 2023. Date of publication 29 March 2023; date of current version 19 April 2023. This work was supported in part by the European Union under Grant 825453 [Micro assembled Terabit/s capable optical transceivers for Datacom applications (CALADAN)] and Grant 871345 [Photonics Solutions at Pilot Scale for Accelerated Medical Device Development (MedPhab)] and in part by the Science Foundation Ireland (SFI) Grants under Grant 12/RC/2276_P2 and Grant 15/IA/2864. *(Corresponding author: Jing Zhang.)*

Jing Zhang, Laurens Bogaert, Geert Morthier, and Gunther Roelkens are with the Photonics Research Group, Department of Information Technology, Ghent University-imec, 9052 Ghent, Belgium (e-mail: Jingzhan.Zhang@ugent.be; Laurens.Bogaert@ugent.be; Geert.Morthier@ugent.be; Gunther.Roelkens@ugent.be).

Bahawal Haq was with the Photonics Research Group, Department of Information Technology, Ghent University-imec, 9052 Ghent, Belgium. He is now with GlobalFoundries, 01109 Dresden, Germany (e-mail: bahawal_haq@hotmail.com).

Ruohui Wang is with the School of Physics, Northwest University, Xi'an 710075, China (e-mail: rwang@nwu.edu.cn).

Bozena Matuskova, Johanna Rimböck, and Stefan Ertl are with the EV Group, E. Thallner GmbH, 4782 Sankt Florian am Inn, Austria (e-mail: B.Matuskova@evgroup.com; J.Rimboeck@evgroup.com; S.Ertl@evgroup.com).

Agnieszka Gocalinska, Emanuele Pelucchi, and Brian Corbett are with the Tyndall National Institute, University College, Cork, T12 R5CP Ireland (e-mail: Agnieszka.Gocalinska@tyndall.ie; Emanuele.Pelucchi@tyndall.ie; Brian.Corbett@tyndall.ie).

Joris Van Campenhout, Guy Lepage, and Peter Verheyen are with imec, 3001 Heverlee, Belgium (e-mail: Joris.VanCampenhout@imec.be; Guy.Lepage@imec.be; Peter.Verheyen@imec.be).

Color versions of one or more figures in this letter are available at https://doi.org/10.1109/LPT.2023.3263279.

Digital Object Identifier 10.1109/LPT.2023.3263279

This work is licensed under a Creative Commons Attribution-NonCommercial-NoDerivatives 4.0 License.
For more information, see https://creativecommons.org/licenses/by-nc-nd/4.0/

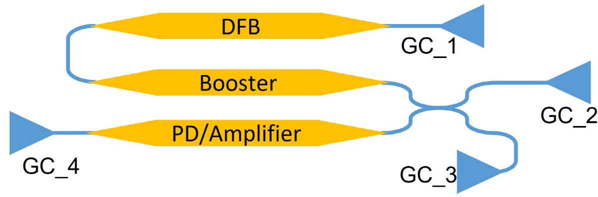

Fig. 1. Schematic of the proposed III-V-on-Si DFB laser with integrated power amplifier.

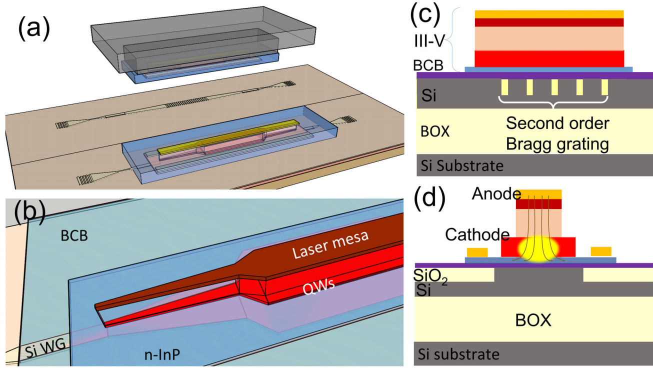

Fig. 2. (a) Transfer printing of a III-V amplifier on the target SiPh circuits, (b) Alignment-tolerant III-V/Si taper structure, (c) Schematic of the C-band III-V-on-Si DFB laser cavity with a second-order Bragg grating patterned in the Si layer, (d) Cross-section and mode profile of the III-V/Si waveguide.

micro-transfer printed DFB laser with co-integrated optical power amplifier using similar pre-fabricated III-V devices, but on Si PICs fabricated in imec's SiPh pilot line. The demonstrated device exhibits single mode operation around 1540 nm, while providing up to 14 dBm waveguide-coupled output power.

II. Design of the III-V-on-Si DFB Laser

The III-V-on-Si DFB laser discussed in this letter consists of a SiPh target chip fabricated at imec using 193nm DUV lithography, and several identical prefabricated III-V amplifiers that are transfer-printed from a III-V source wafer to provide gain to the target chip. The adopted platform for the SiPh circuit features a 400 nm thick crystalline Si device layer with a single 180 nm etch step to define the integrated photonics devices. Furthermore, the trenches alongside these rib waveguides are planarized with SiO_2 through a Chemical-Mechanical Polishing (CMP) process. Fig. 1 shows the proposed III-V-on-Si integrated circuit. It consists of a second-order grating DFB laser, of which one of the outputs is fed to a co-integrated III-V-on-Si power amplifier. The III-V-on-Si device at the bottom can be used either as a photodetector, to detect the back-reflection from the optical system, or as a reference optical amplifier, to evaluate the performance of the integrated power amplifier. The heterogeneous integration of the III-V devices with the SiPh circuit is realized by μTP an array of identical prefabricated III-V amplifier coupons onto the SiPh integrated circuits.

The prefabricated III-V amplifier is 1140 µm long and consists of a straight waveguide section with 180 µm long alignment-tolerant III-V taper structures present at both sides of a 780 µm long straight III-V rib waveguide. The overall length of the device coupon is 1180 µm. These III-V/Si tapers couple the light efficiently from the laser cavity to the underlying Si waveguide while offering robustness to the alignment accuracy levels provided by the μTP process. While the same III-V coupon is used for constructing the laser and the co-integrated power amplifier, the underlying silicon photonics waveguide layout will be different.

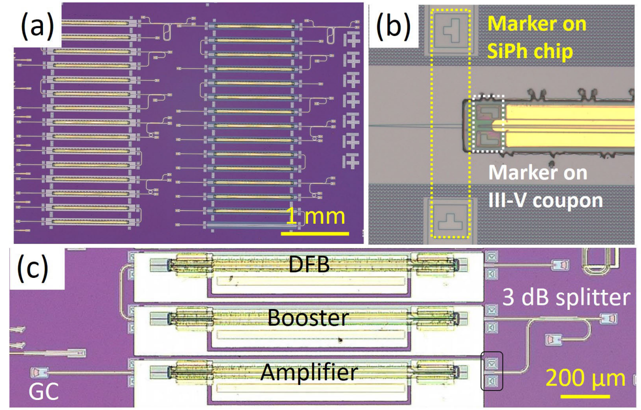

Fig. 3. (a) A SiPh chip with an array of transfer-printed C-band amplifiers, (b) Microscope image of the fiducial alignment markers. (c) Resulting III-V-on-Si integrated circuit after the deposition of metal contact pads.

The DFB laser cavity is formed by a III-V/Si hybrid waveguide, where a uniform second-order Bragg grating is patterned on a 4.5 µm wide Si rib waveguide, as shown in Fig. 2(c). The length, period and duty cycle of this Bragg grating are 600 µm, 475 nm and 75%, respectively. The cross-section of the III-V/Si waveguide is shown schematically in Fig. 2(d), with a p-cladding mesa width and an active region width of respectively 3.2 µm and 4.8 µm, for the adopted amplifier coupons. As the grating is realized by a 180 nm etch from the top of Si waveguide, the effective index of the corrugated silicon waveguide is significantly reduced such that the optical mode is mostly confined in the III-V active region, as depicted in Fig. 2(d). By using a wide Si waveguide in combination with a narrow p-mesa and given a high alignment accuracy provided by the μTP system, the guided optical mode would not be impacted by the lateral misalignment. Furthermore, higher order guided modes are expected to have high propagation losses due to the sidewall roughness of the III-V waveguide and less efficient pumping of the active region outside the p-mesa, which allows to achieve single transverse mode (fundamental TE mode) operation. The co-integrated power amplifier and photodetector/amplifier on the other hand are printed on top of a continuous 3 µm wide Si rib waveguide

The fabrication and release of the III-V SOA coupons are described in detail in [5]. Prior to the printing step, the SiPh chips are spray-coated with a 100 nm thick DVS-BCB adhesive layer. After a short soft bake at 150 °C the sample is ready for the laser integration. Micro-transfer printing of the III-V amplifiers on the SiPh target chip was carried out using a Polydimethylsiloxane (PDMS) stamp with a single post of 40 µm × 1200 µm, as illustrated in Fig. 2(a) and (b). Fig. 3(a) shows a target SiPh chip with two arrays of transfer-printed III-V SOAs with a 280 µm pitch. A set of fiducial markers, as shown in Fig. 3(b), are used to facilitate the automatic align-

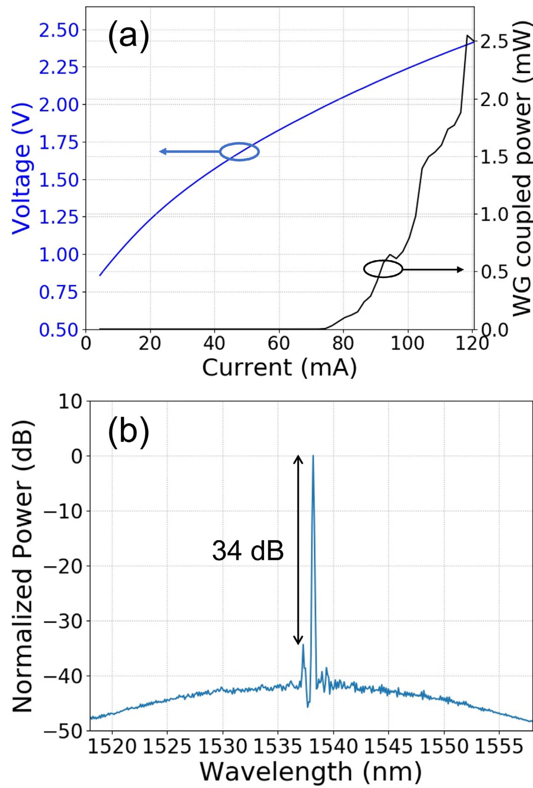

Fig. 4. (a) Light-current-voltage for the integrated III-V-on-Si DFB laser without power amplifier. The plotted optical power is the single-side waveguide-coupled power at GC_1 after calibrating out the insertion loss of the grating coupler. (b) DFB laser spectrum measured at 100 mA DFB laser bias current.

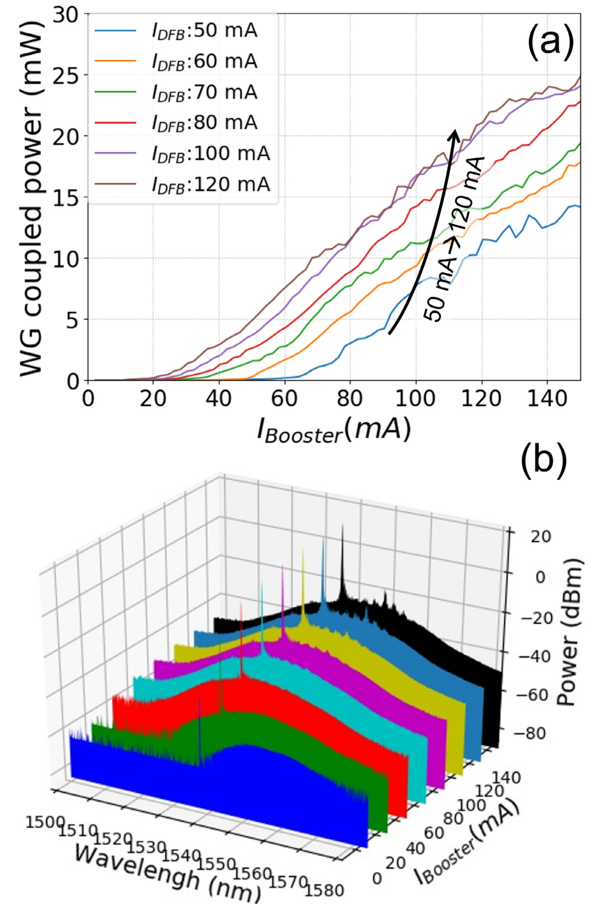

Fig. 5. (a) Waveguide-coupled output power of the III-V-on-Si DFB laser with co-integrated power amplifier as a function of power amplifier current and DFB laser bias current. (b) A set of laser spectra for different power amplifier bias currents with the DFB laser bias current fixed at 100 mA.

ment by using a pattern recognition function integrated in the μTP system. After the μTP process, a few simple steps such as photoresist encapsulation removal, BCB curing and metal deposition are performed to enable electrical interfacing to the device. Fig. 3(c) shows the resulting III-V-on-Si integrated circuits.

III. Characterization

To characterize the fabricated device, a setup consisting of two vertical optical fiber probes, 2 Keithley current sources, and 4 DC probes were used. The temperature-controlled stage was set to 20 °C. First, the performance of the stand-alone DFB laser was assessed by aligning a fiber probe to GC_1, thereby collecting the laser output power (Fig. 1). The fiber probe GC_1 was then connected to a 99:1 splitter, where the 99% branch was fed to an optical spectrum analyzer (OSA, YOKOGAWA AQ6375), whereas the 1% branch was connected to an optical power meter (HP 8163A). Fig. 4(a) shows the obtained light-current-voltage (LIV) curves of the stand-alone DFB laser (without operating the power amplifier), where the differential resistance reduces with the increase of bias current and goes down to 9 Ω at 100 mA. The waveguide-coupled power is obtained by calibrating out the insertion loss of the grating coupler (8 dB at the operation wavelength) and the splitting loss of the 99:1 splitter at the operation wavelength. Based on this light-current (LI) curve, it is clear that the threshold of the DFB laser is below 80 mA, which corresonds to a threshold current density of 2.36 kA/cm^2. The waveguide-coupled power can reach up to 4 dBm at 120 mA. Fig. 4(b) shows a representative laser spectrum at a bias current of 100 mA, indicating that the device exhibits single mode operation around 1540 nm with 34 dB side-mode-suppression-ratio (SMSR).

After verifying the performance of the stand-alone DFB laser, the co-integrated power amplifier was turned on and biased simultaneously with the DFB laser. To evaluate the laser-power amplifier combination, the fiber probe was aligned to collect power from GC_2. Fig. 5(a) shows a set of measured waveguide-coupled output powers as a function of the power amplifier bias current for different DFB laser bias currents. Similar to the standalone DFB laser measurements, these values are presented after calibration of grating coupler and splitter losses, where the latter now not only includes the external 99:1 splitter but also the integrated 3 dB splitter. When applying a total current of 270 mA (120 mA to DFB laser and 150 mA to power amplifier), 14 dBm waveguide-coupled power was obtained. Furthermore, it was found that the DFB laser was even able to lase below the threshold current of the standalone cavity when the power amplifier was biased at a high current level. This is due to parasitic reflections that form a compound laser cavity with the DFB laser and the power amplifier inside. Because of these parasitic reflections and the

misalignment of the operation wavelength to the gain peak, which is around 1550 nm, the SMSR reduces to 28 dB at maximum output power. Higher output power and improved SMSR are expected when the laser can be operated around the gain peak, which can be realized by slightly increasing the Bragg grating period.

IV. Conclusion

For the first time, we demonstrate a III-V-on-Si integrated DFB laser with a co-integrated optical power amplifier by μTP an array of identical prefabricated InP-based SOAs on a SiPh integrated circuit. The SOA coupons were fabricated on the InP source substrate in dense arrays with 70 μm vertical pitch, such that the expensive InP source material is used as efficiently as possible, whereas the device pitch of these SOAs after printing on the target SiPh chip is 280 μm. The resulting stand-alone DFB laser exhibits single mode operation around 1540 nm with 4 dBm waveguide-coupled power and a SMSR of 34 dB. After enabling the amplification provided by the co-integrated optical power amplifier, the output power in the waveguide reaches up to 14 dBm, at the cost of a slightly reduced SMSR of 28 dB. It is expected that both the maximum output power and SMSR can be improved by readjusting the Bragg grating period to bring the lasing wavelength closer to the gain peak.

In this letter, we demonstrate an example of how μTP can help augment the standard SiPh platforms to realize more versatile III-V-on-Si integrated circuits. μTP is suited to realize complex PICs by intimately (co-)integrating a variety of non-native optical and (high-speed) electronic components, which can be released from their native substrates and brought together on a single target chip. Furthermore, μTP allows to do this heterogeneous integration in a massively parallel manner on a 200/300 mm wafer such that the cost of the resulting III-V-on-Si PICs can be significantly reduced.

References

[1] Europractice. *Photonic Integrated Circuit Prototyping and Small Volume Production*. [Online]. Available: https://www.imecint.com/sites/default/files/imported/Photonic%5C%2520integrated%5C%2520circuit_EN_v4_MPW_yi_0.pdf

[2] R. Jones, "Overview and future challenges on III-V integration technologies in silicon photonics platform," in *Proc. Opt. Fiber Commun. Conf. Exhib. (OFC)*, 2021, pp. 1–3.

[3] J.-S. Park, M. Tang, S. Chen, and H. Liu, "Monolithic IIIV quantum dot lasers on silicon," in *Semiconductor Nanodevices* (Frontiers of Nanoscience), vol. 20, D. A. Ritchie, Ed. Amsterdam, The Netherlands: Elsevier, 2021, pp. 353–388. [Online]. Available: https://www.sciencedirect.com/science/article/pii/B9780128220832000095

[4] B. Corbett et al., "Transfer printing for silicon photonics," in *Semiconductors and Semimetals*, vol. 99. Amsterdam, The Netherlands: Elsevier, 2018, pp. 43–70.

[5] B. Haq et al., "Micro-transfer-printed III-V-on-silicon C-band semiconductor optical amplifiers," *Laser Photon. Rev.*, vol. 14, no. 7, 2020, Art. no. 1900364.

[6] J. Goyvaerts et al., "Enabling VCSEL-on-silicon nitride photonic integrated circuits with micro-transfer-printing," *Optica*, vol. 8, no. 12, p. 1573, 2021.

[7] A. Osada, Y. Ota, R. Katsumi, K. Watanabe, S. Iwamoto, and Y. Arakawa, "Transfer-printed quantum-dot nanolasers on a silicon photonic circuit," *Appl. Phys. Exp.*, vol. 11, no. 7, Jun. 2018, Art. no. 072002, doi: 10.7567/APEX.11.072002.

[8] C. Li et al., "Transfer printed, vertical GaN-on-silicon micro-LED arrays with individually addressable cathodes," *IEEE Trans. Electron Devices*, vol. 69, no. 10, pp. 5630–5636, Sep. 2022.

[9] J. Goyvaerts et al., "Transfer-print integration of GaAs p-i-n photodiodes onto silicon nitride waveguides for near-infrared applications," *Opt. Exp.*, vol. 28, p. 21275, Jul. 2020.

[10] J. Zhang et al., "Silicon photonics fiber-to-the-home transceiver array based on transfer-printing-based integration of III-V photodetectors," *Opt. Exp.*, vol. 25, p. 14290, Jun. 2017.

[11] Y. Wang, G. Li, X. Gu, Y. Kong, Y. Zheng, and Y. Shi, "Responsibility optimization of a high-speed InP/InGaAs photodetector with a back reflector structure," *Opt. Exp.*, vol. 30, no. 4, pp. 4919–4929, Feb. 2022. [Online]. Available: https://opg.optica.org/oe/abstract.cfm?URI=oe-30-4-4919

[12] F. Yu et al., "High-power high-speed MUTC waveguide photodiodes integrated on Si_3N_4/Si platform using micro-transfer printing," *IEEE J. Sel. Topics Quantum Electron.*, vol. 29, no. 3, pp. 1–6, May 2023.

[13] N. Ye et al., "Transfer print integration of waveguide-coupled germanium photodiodes onto passive silicon photonic ICs," *J. Lightw. Technol.*, vol. 36, no. 5, pp. 1249–1254, Mar. 1, 2018.

[14] S. Cuyvers et al., "High-yield heterogeneous integration of silicon and lithium niobate thin films," in *Proc. Conf. Lasers Electro-Opt. (CLEO)*, May 2022, pp. 1–2.

[15] T. Vanackere et al., "Micro-transfer printing of lithium niobate on silicon nitr," in *Proc. Eur. Conf. Opt. Commun. (ECOC)*, Dec. 2020, pp. 1–4.

[16] Z. Li et al., "Photonic integration of lithium niobate micro-ring resonators onto silicon nitride waveguide chips by transfer-printing," *Opt. Mater. Exp.*, vol. 12, no. 11, pp. 4375–4383, Nov. 2022. [Online]. Available: https://opg.optica.org/ome/abstract.cfm?URI=ome-12-11-4375

[17] R. Loi et al., "Micro transfer printing of electronic integrated circuits on silicon photonics substrates," in *Proc. Eur. Conf. Integr. Opt. (ECIO)*, Milano, Italy, 2022, Paper F.C.3.

[18] J. Zhang et al., "Transfer-printing-based integration of a III-V-on-silicon distributed feedback laser," *Opt. Exp.*, vol. 26, no. 7, pp. 8821–8830, Apr. 2018. [Online]. Available: https://opg.optica.org/oe/abstract.cfm?URI=oe-26-7-8821

[19] B. Haq et al., "Micro-transfer-printed III-V-on-silicon C-band distributed feedback lasers," *Opt. Exp.*, vol. 28, no. 22, p. 32793, 2020.